https://doi.org/10.5194/hess-2024-240
Preprint. Discussion started: 23 September 2024

Hydrology and Earth System Sciences
Discussions

Self-potential signals related to tree transpiration in a Mediterranean climate

Kaiyan Hu[1], Bertille Loiseau[2], Simon D. Carrière[2], Nolwenn Lesparre[3], Cédric Champollion[4], Nicolas K. Martin-StPaul[5], Niklas Linde[6], Damien Jougnot[2]

[1]Department of Applied Geophysics, School of Geophysics and Geomatics, China University of Geosciences, Wuhan 430074, China
[2]Sorbonne Université, CNRS, EPHE, UMR 7619 METIS, F-75005 Paris, France
[3]Université de Strasbourg, CNRS, EOST, ENGEES, ITES UMR 7063, 67000 Strasbourg, France
[4]Université de Montpellier, UMR 5243 GM (CNRS/UM/UA), Montpellier, France
[5]URFM, INRAE, Domaine Saint Paul, Site Agroparc, 84000 Avignon, France
[6]Institute of Earth Sciences, University of Lausanne, 1015 Lausanne, Switzerland

Correspondence to: Damien Jougnot (damien.jougnot@upmc.fr)

Abstract. Transpiration is a crucial process in the water cycle and its quantification is essential for understanding terrestrial ecosystem dynamics. Solely relying on sap flow measurements may not fully assess tree transpiration due to its complexity. Self-potential (SP), a passive geophysical method, may provide constraints on transpiration rates even if many questions remain about tree electrophysiological effects. In this study, we continuously measured tree SP and sap velocity on three tree species for one year in a Mediterranean climate. Using wavelet coherence analysis and variational mode decomposition, we explored the empirical relationship between tree SP and transpiration. Our analysis revealed strong coherence between SP and sap velocity at diurnal time scales, with coherence weakening and phase shifts increasing on days with higher water supply. We estimated electrokinetic coupling coefficients using a linear regression model between SP and sap velocity variations at the diurnal scale, resulting in values typically found in porous geological media. During a dry growing season, the electrokinetic effect emerges as the primary contribution to tree SP, indicating its potential utility in assessing transpiration rates. Our results emphasize the need for improved electrode configurations and physiochemical modeling to elucidate tree SP in relation to transpiration.

1 Introduction

Climate change and anthropogenic activities exert significant influence on terrestrial ecosystems, particularly impacting vegetation (Mottl et al., 2021; Nolan et al., 2018). In anticipation of these growing impacts, understanding the effects of phenomena such as droughts on forests is essential (Anderegg et al., 2016). Evapotranspiration (ET) stands as a critical component of the water cycle, accounting for approximately 65 % of precipitated water at the continental scale (Fisher et al.,

https://doi.org/10.5194/hess-2024-240
Preprint. Discussion started: 23 September 2024


Hydrology and Earth System Sciences Discussions

2017; Oki and Kanae, 2006). Transpiration, constituting approximately 50 % of global terrestrial evapotranspiration (Bachofen et al., 2023; Jasechko et al., 2013; Kuang et al., 2024; Schlesinger and Jasechko, 2014; Wei et al., 2017), can reach 95 % in tropical forests during dry seasons (e.g., Kunert et al., 2017). Monitoring of transpiration is crucial for enhancing our understanding of plant-water relations, ecohydrological processes, and water resource management, with implications for agriculture, ecology, and climate science. Its quantification often relies on sap flow measurements (Granier, 1987; Poyatos et al., 2016; Smith and Allen, 1996) with heat dissipation techniques being widely used due to their ease of implementation, continuous measurements, and high precision (Flo et al., 2019; Poyatos et al., 2021; Wang et al., 2023). However, these methods represent point measurements, rather than integrated responses across the entire stem (Flo et al., 2019; Oliveras, and Llorens 2001).

In recent years, geophysical methods have gained considerable attention for studying ecohydrological systems (e.g., Carrière et al., 2021a, b; Dumont and Singha, 2024; Harmon et al., 2021; Hermans et al., 2023; Jayawickreme et al., 2014; Loiseau et al., 2023; Luo et al., 2020; Voytek et al., 2019). Among geophysical methods, the passive self-potential (SP) method has potential for estimating sap velocity (Gibert et al., 2006; Gindl et al., 1999;). Measurable SP signals naturally occur between trees and the surrounding soil in response to bioelectrical effects within plants. Tree SP measurements are often positive when measuring the voltage difference of the stem with respect to the surrounding soil, the so-called biopotentials (e.g., Fensom, 1957, 1963; Gibert et al., 2006; Tattar and Blanchard, 1976; Zapata et al., 2020). Tree transpiration processes, which facilitate water and solute transport within the xylem and phloem of trees, trigger electrokinetic and electro-diffusive effects, leading to the generation of biopotentials and, hence, measurable SP signals. In theory, SP signals provide an integrated response between the two electrodes that is sensitive to the transpiration process.

SP signals are often measured by non-polarizable electrodes and a high-impedance voltmeter to avoid current leakage arising from the measurements. Due to their stability, non-polarizing Ag/AgCl electrodes have been used to measure SP signals within the trunk in laboratory experiments (e.g., Gil and Vargas, 2023; Gindl et al., 1999; Oyarce and Gurovich, 2010). However, this kind of electrodes contains gels or electrolytes that dry up after one to two months for small-sized electrodes, thereby, leading to erroneous measurements (Fensom, 1963). Such electrodes are hence deemed impractical for prolonged, continuously monitored field experiments. Hubbard et al. (2011) developed a miniaturized Petiau-type $Pb/PbCl_2$ electrode (Petiau, 2000) for measuring SP induced by a biogeobattery within a small laboratory column, potentially offering a suitable solution with an extended lifespan. However, its installation presents challenges, particularly in shallow depths beneath bark and to ensure effective contact with the sapwood. Instead, in outdoor natural environment, polarizable stainless metal electrodes are often used for tree SP measurements (e.g., Fensom, 1963; Gibert et al., 2006; Le Mouël et al., 2024; Zapata et al., 2020, 2021). A non-polarizing electrode is one in which the electrode potential is independent of the current passing through the circuit. However, in both polarizable and non-polarizing electrodes, electrode-related effects are superimposed on the primary effects of interest, often leading to observations that are difficult to interpret. The electrode potentials depend on the electrode design, the temperature, the surrounding and internal hydrochemical environments (Jougnot and Linde, 2013). Due to electrode-related effects, the measured electrical voltage shows often important drifts during long-term monitoring,

https://doi.org/10.5194/hess-2024-240
Preprint. Discussion started: 23 September 2024


Hydrology and Earth System Sciences
Discussions

related for instance to electrode aging (e.g., Perrier et al., 1997; Hu et al., 2020). Hao et al. (2015) conducted experiments to measure plant-related voltages using electrodes made of different metals and found differences exceeding 10 mV when using copper electrodes with 5 mm differences in diameter. When employing metal electrodes to measure SP on trees, it is hence crucial to ensure consistency in terms of electrode design (materials and geometry). Consequently, the installation and the choice of electrodes used to measure tree SP should be made very carefully.

Even in the absence of electrode effects, the interpretation of tree-SP signals is complicated due to the different mechanisms contributing to the observed data. These include both electrokinetic and electrochemical processes occurring within the sapwood (Fensom, 1957; Fromm and Lautner, 2007, 2012; Gibert et al., 2006; Gil and Vargas, 2023; Love et al., 2008; Tattar and Blanchard, 1976). Moreover, Barlow (2012) and Le Mouël et al. (2024) suggest that luni-solar tides could induce electric fields, possibly further complicating the interpretation of SP measurements on trees. However, some long-term measurements have not observed clear monthly patterns related to lunar cycles (e.g., Fensom, 1963, Zapata et al., 2021). Uncertainties surrounding these mechanisms make quantitative interpretations of SP data in terms of the water dynamic within the soil-plant system very challenging.

Given the considerable ambiguity surrounding the mechanisms governing the coupling magnitude, which determines the mathematical relationship between SP and sap flow observations, further experimentation is essential to clarify their correlation *in situ*. The existing literature on plant-related SP predominantly focuses on individual trees (Belashev, 2024; Gibert et al., 2006; Hao et al., 2015; Le Mouël et al., 2010; Voytek et al., 2019) or different tree species, often with non-continuous or short-term measurements (e.g., Gil and Vargas, 2023; Oyarce and Gurovich, 2010; Pozdnyakov, 2013; Zapata et al., 2020). Recently, Le Mouël et al. (2024) analyzed SP signals from various trees using the singular spectrum decomposition method, suggesting that sap flow and multi-scale tree SP may be partially or entirely induced by terrestrial gravitational tides, although without providing data on sap flow. Several pertinent questions remain unanswered regarding tree SP observations: (1) Do different tree species exhibit distinct time-varying SP patterns under identical environmental conditions? (2) Do trees of the same species display SP characteristics that depend on the weather conditions? (3) Will two trees of the same species show similar SP responses to sap velocity? (4) Is SP a reliable indicator of sap velocity within the trunk? (5) When are electrokinetic effects dominating tree SP responses?

To address these questions, we review tree SP theory in Section 2, followed by a description of long-term SP monitoring experiments conducted at three distinct sites in the French Mediterranean region, along with an outline of data analysis methods in Section 3. In Section 4.1, we present and analyze the data obtained from measurements on four different trees at three sites. Sections 4.2 and 4.3 investigate the short-term characteristics of tree SP in terms of correlations with sap velocity, precipitation, evapotranspiration, and other meteorological data.

https://doi.org/10.5194/hess-2024-240
Preprint. Discussion started: 23 September 2024

Hydrology and Earth System Sciences
Discussions

2 Theoretical background concerning tree SP

Pioneering research of tree SP monitoring dates back to the early 1960s, when Fensom (1963) embarked on extensive studies to monitor SP on different trees. Earlier studies of the bioelectrical potential can be found in Fensom (1957). Fensom (1963) observed that the electrical voltages were the strongest during growing seasons and proposed that voltage measurements of plants might detect cambial growth. Subsequent studies by Gindl et al. (1999) measured both sap velocity and SP on tree stems in a well-controlled laboratory experiment, uncovering a significant linear correlation between the two. They suggested that the transpiration process acts as a driving force in xylem sap, generating electrokinetic effects that explain the relationship between the sap velocity and SP data, suggesting the potential value of using SP data to estimate plant sap flow. Through continuous observations of an individual poplar tree at various heights and positions, Gibert et al. (2006) found that the relationship between the SP and the sap-flow velocity is not entirely linear. They suggested the presence of electrically active structures within the xylem leading to electro-diffusive effects within plants. Voytek et al. (2019) simulated the SP generated by root water uptake and reconstructed the observed time-varying patterns of SP in the root zone, confirming that plant root water uptake affects the observed electrical voltages. However, the numerical simulations accounting for the electrokinetic coupling process induced by the soil water movement in the root zone could not predict the amplitude of the observed SP.

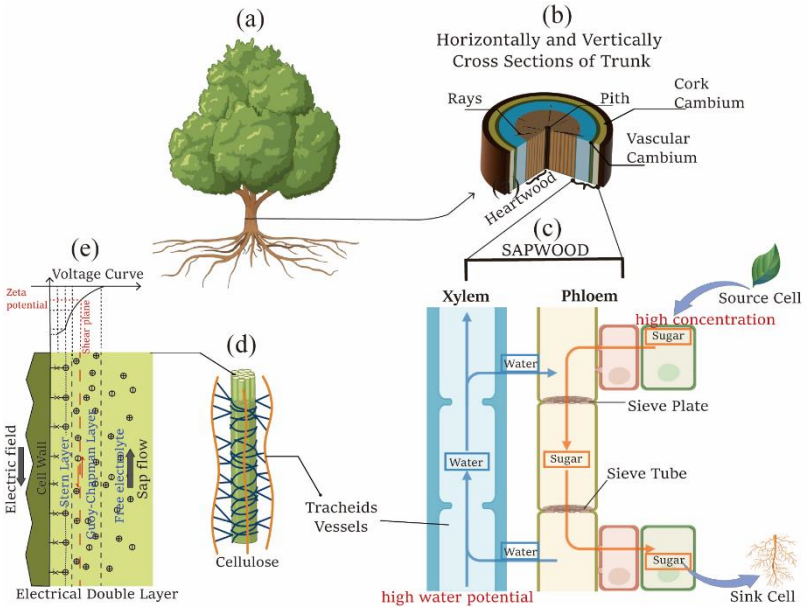

Figure 1: Schematic diagram of tree SP: (a) Adapted tree illustration from "Ash tree" by BioRender.com (2024); (b) Horizontally and vertically cross sections of trunk; (c) Vertically extracted xylem and phloem adapted from "Plant Vessels Layout" by BioRender.com (2024); (d) Cellulose structure adapted from "Cell wall (cellulose)" by BioRender.com (2024); (e) Electrical double layer.

Previous experimental studies on SP between the living plant and the surrounding soil have shown that the electrical voltages generated by physiological, physical, and chemical processes can range from tens to hundreds of millivolts (e.g., Fensom, 1963; Pozdnyakov, 2013; Zapata et al., 2020). These magnitudes are comparatively high compared to SP signals generated by

https://doi.org/10.5194/hess-2024-240
Preprint. Discussion started: 23 September 2024


Hydrology and Earth System Sciences
Discussions

near-surface water or solute flux (e.g., Jougnot et al., 2015; Voytek et al., 2019; Hu et al., 2020). A schematic diagram of a tree is presented in Fig.1 to summarize the mechanisms of SP generation. SP differences from root to shoot are induced within the sapwood, including the xylem and phloem (Figs. 1b&c). Below, we describe the possible mechanisms generating tree SP.

2.1 Self-potential signals generated by xylem and phloem transport

Observed SP signals arise from the superposition of contributions arising from different coupling sources and from electrode-related effects (e.g., Hu et al., 2020; Jougnot et al., 2015; Jougnot and Linde, 2013;). The SP signal due to flow and mass transport process can be described by the following Poisson equation in absence of external electrical current:

$$\nabla \cdot (-\sigma \mathbf{E}) = \nabla \cdot (\mathbf{J}_{\text{ek}} + \mathbf{J}_{\text{diff}}), \quad (1)$$

where σ (S m^{-1}) is the bulk electrical conductivity; $\mathbf{E} = -\nabla V$ (V m^{-1}) is the electrical field; ∇V is the electrical potential gradient; $\mathbf{J}_{\text{ek}}$ (A m^{-2}) and $\mathbf{J}_{\text{diff}}$ (A m^{-2}) are the electrokinetic and electro-diffusive current density, respectively. We detail these two contributions below.

The primary contribution of sap ascent occurs in the xylem, where vessels transport water and dissolved minerals from the roots throughout the plant. This process relies on transpiration pulling, creating a negative pressure gradient that drives upward flow through the xylem (Fig. 1c). The xylem vessels feature a capillary-like structure, as illustrated in Fig. 1d. Although the cellulose walls of the xylem are electrically neutral and insulating, they become negatively charged as they attract water molecules (Fensom, 1957). According to the electrokinetic mechanism in presence of an electrical double layer, the upward flow of sap induces a natural electric field in the opposite direction, as depicted in Fig. 1e.

The electrokinetic cross-coupling coefficient C_{ek} (V Pa^{-1}) is defined as the ratio of voltage difference $V_{z1} - V_{z2}$ to pressure difference $p_{z1} - p_{z2}$ with no external currents (i.e., electrical flux equals 0). The C_{ek} is determined using the Helmholtz-Smoluchowski (HS) equation:

$$C_{\text{ek}} = \frac{V_{z1} - V_{z2}}{p_{z1} - p_{z2}}\Big|_{\mathbf{J}=\mathbf{0}} = \frac{\epsilon_{\text{f}} \zeta}{\sigma_{\text{f}} \eta_{\text{f}}}, \quad (2)$$

where ϵ_{f} (F m^{-1}) and σ_{f} (S m^{-1}) denote the dielectric permittivity and the electrical conductivity of the capillary fluid, respectively. The parameter ζ (V) is the Zeta potential at the shear plane of the electrical double layer (Fig. 1e); it typically has a negative sign. Both σ_{f} and ζ are influenced by temperature and ion concentration. Consequently, the voltage induced by xylem transport not only depends on sap velocity but also on sap temperature and concentration. Based on laboratory experiments under different pore water ionic concentrations, Linde et al., (2007) proposed an empirical relationship between the logarithm of C_{ek} and σ_{f}. A similar model could be devised to estimate C_{ek} within vascular plants.

Alternatively, the electrokinetic current density $\mathbf{J}_{\text{ek}}$ (A m^{-2}) can be expressed by the product of the effective excess charge density $\hat{Q}_v$ (C m^{-3}) and the Darcy velocity $\mathbf{u}$ (m s^{-1}) (e.g., Jougnot et al., 2020):

$$\mathbf{J}_{\text{ek}} = \hat{Q}_v \mathbf{u}. \quad (3)$$

https://doi.org/10.5194/hess-2024-240
Preprint. Discussion started: 23 September 2024


Hydrology and Earth System Sciences
Discussions

Here, $\hat{Q}_v$ indicates the density of excess charge in the diffuse layer of electrical double layer model (Fig. 1e) that is effectively dragged by sap flow. Following Kormiltsev et al. (1998) and Jougnot et al. (2019), C_{ek} can be transformed into $\hat{Q}_v$ by

$$\hat{Q}_v = -\frac{\eta_{\mathrm{f}}\sigma}{k} C_{\mathrm{ek}}, \tag{4}$$

where k (m^2) denotes permeability. Based on Eq. (1), in absence of external electric currents and under the assumption of 1-D flow, the equivalent current density induced by the sap flow can be simplified to:

$$\sigma \mathbf{E} = -\sigma \nabla V = -\hat{Q}_v \mathbf{u}. \tag{5}$$

Thus, the $\hat{Q}_v$ can be expressed as (e.g., Jougnot et al., 2012)

$$\hat{Q}_v = \frac{\sigma \nabla V}{\mathbf{u}}. \tag{6}$$

During the transpiration process, water loss coupled with osmotic changes lead to an increase in solute concentration towards the crown. This implies the potential generation of electro-diffusive potentials due to electrochemical differences. Common ion species found in plants include protons (H^+), calcium (Ca^{2+}), potassium (K^+), magnesium (Mg^{2+}), ammonium (NH^{4+}), chlorine (Cl^-), nitrate (NO^{3-}), among others (Davies, 2006; Miller and Wells, 2006; Volkov and Markin, 2012). For instance, increases in K^+ of xylem sap occur with increasing transpiration demand and consequently increase hydraulic conductivity and capacity of water movement (e.g., Losso et al., 2023; Nardini et al., 2011). However, the concentration distribution along the longitudinal direction exhibits different trends and patterns among various tree species (McDonald et al., 2002). The electro-diffusive current density $\mathbf{J}_{\mathrm{diff}}$ ($A\ m^{-2}$) arises from the electrochemical potential gradient, influenced by the activities of different ion species:

$$\mathbf{J}_{\mathrm{diff}} = -\frac{\mathrm{k_B} T_{\mathrm{K}}}{\mathrm{e_0}} \sigma \sum_{i=1}^{N} \frac{t_i^{\mathrm{H}}}{q_i} \nabla \ln a_i, \tag{7}$$

where a_i, t_i^{H} and q_i represent the activity (i.e. thermodynamically effective concentration), the microscopic Hittorf transport number, and the valence of the ion species i, respectively; $\mathrm{k_B}$ ($K\ J^{-1}$), $\mathrm{e_0}$ (C), T_{K} (K), and σ ($S\ m^{-1}$) are the Boltzmann constant, the elementary charge, the temperature and bulk electrical conductivity; N is the total number of ion species in xylem sap. The equivalent electrical potentials induced by $\mathbf{J}_{\mathrm{diff}}$ is expressed by

$$\nabla \varphi_{\mathrm{diff}} = \frac{\mathbf{J}_{\mathrm{diff}}}{\sigma} = -\frac{\mathrm{k_B} T_{\mathrm{K}}}{\mathrm{e_0}} \sum_{i=1}^{N} \frac{t_i^{\mathrm{H}}}{q_i} \nabla \ln a_i. \tag{8}$$

Compared with the electro-diffusive effect, cell membrane potentials across xylem tracheids constitute another source of electrical potential gradient (Fensom, 1957; Hedrich and Schroeder, 1989). Further details on the membrane potential can be found in Nobel (2009) and Spanswick (2006).

Water movement within the xylem is mainly sustained by hydrostatic pressure gradients driven by transpiration processes. Conversely, in the phloem, water flow is influenced not only by hydrostatic pressure gradients but also by osmotic pressures resulting from translocation processes. Specifically, the loading of sugars into the phloem leads to an increase in solute concentration but a decrease in water potential in source cells, creating a higher water potential in sink cells (Fig. 1c).

https://doi.org/10.5194/hess-2024-240
Preprint. Discussion started: 23 September 2024


Hydrology and Earth System Sciences
Discussions

Consequently, water and solutes move upward in the xylem and downward in the phloem (Hölttä et al., 2006). Moreover, osmotic pressures in the phloem cause water from the xylem to radially flow into the phloem (Fig. 1c). Apart from the passive electrokinetic and electro-diffusive mechanisms, actively transporting charged particles into cells may lead to the accumulation of internal electrical potential and the occurrence of electrogenic pumps across membranes (Nobel, 2009).

2.2 Previous studies and discussion of tree SP generation

Multiple studies have explored the relationship between sap flow and electrical potential differences along plant stems, often attributing it to electrokinetic effects (e.g., Gindl et al., 1999; Gil and Vargas, 2023; Gibert et al., 2006; Fensom, 1963; Koppán et al., 2002). However, this explanation has come under scrutiny due to inconsistencies observed in measurements. Love et al. (2008) conducted a laboratory experiment involving *Ficus benjamina* trees and their surrounding soil for different pH levels. They proposed that disparities in electrical potential differences between the plant and its surrounding soil are predominantly influenced by the pH difference between the xylem and the soil. Similarly, Zapata et al. (2020), based on measurements from various trees in a Mediterranean forest region, suggested to abandon the electrokinetic mechanism to explain SP differences along the trunk. However, their measurements were conducted over a limited period. Furthermore, fluctuations in pH alter the concentrations of H^+ and OH^- ions in aqueous solutions, consequently affecting the Zeta potential of the electrical double layer model (e.g., Al Mahrouqi et al., 2017; Leroy et al., 2013). As a result, pH variations contribute to changes in the electrokinetic coupling coefficients and the magnitudes of corresponding SP.

Aside from the observed longitudinal differences in electrical potential, measurements taken across the stem's cross-sectional profile reveal distinct radial polarization (Isam et al., 2017; Zapata et al., 2020). Isam et al. (2017) conducted measurements of short-circuit currents radially along the trunk's growth direction, noting a peak current near the vascular cambium—a layer between the secondary xylem and phloem (refer to Fig. 1b). They observed strong electrical current generation may result from the low electrical resistance of living tissues, the influx of water into the phloem, and the diffusion of charges around the cambium region. These findings suggest that the measured tree SP varies also with respect to the depth at which electrodes are inserted into the trunk.

As the measured SP is influenced by multiple mechanisms, its composition changes with water and solute movements, exhibiting spatial and temporal variations. Interpreting tree SP observations becomes complex due to these multifaceted mechanisms, which exhibit different patterns under various seasonal and meteorological conditions. Rather than relying on a single generative mechanism and short-term observations, we present below results obtained from continuous, long-term monitoring of tree SP, sap velocity, and meteorological data to comprehensively analyze their correlations over time.

https://doi.org/10.5194/hess-2024-240
Preprint. Discussion started: 23 September 2024

Hydrology and Earth System Sciences
Discussions

3 Materials and Methods

3.1 Study sites and trees

Three distinct experimental sites were selected in the French Mediterranean region to monitor sap velocity and SP on four trees from three different species (Fig. 2). The characteristics of each site are summarized in Table 1. All sites are located into karstic hydro-systems. The Larzac and LSBB test sites are part of the H+ national observatory service and the OZCAR research infrastructure (Gaillardet et al. 2018), while the Font-Blanche site belongs the ICOS research infrastructure (Gielen et al., 2017).

Table 1 Features of experimental sites and trees

Sites / Property	Larzac	LSBB	Font-Blanche	
Tree number	C2	A3	P327	C325
Acronyms	LaQp	LSQi	FBPh	FBQi
Tree species	Pubescent oak (*Quercus pubescens*)	Holm oak (*Quercus ilex L.*)	Aleppo pine (*Pinus halepensis Mill.*)	Holm oak (*Quercus ilex L.*)
Circumference of trunk (m)	0.900	0.428	1.083	0.396
Xylem anatomy	Ring-porous	Ring-porous	Diffuse-porous	Ring-porous
Electrical resistivity of sapwood ($\Omega \cdot m$)	282	/	369	250
Bed rock	Dolomite	Limestone	Limestone	
Mean altitude (m)	708	422	425	
Soil depth (m)	0-80	0-70	0-60	
Mean annual precipitation (mm)	870	900	650	
Mean annual evapotranspiration (mm)	600	580	460	
Mean annual temperature (°C)	10.5	13	14	

The Font-Blanche Forest, located 30 km east of Marseille and approximately 7 km from the coastline (Fig. 2a), sits at an elevation of 425 m (Ollivier et al., 2021). The bedrock consists of sub-recifal Cretaceous limestone with Urgonian facies. The forest is dominated by Aleppo pines (*Pinus halepensis Mill.*), averaging 13 m in height, with an understory of Holm oaks (*Quercus ilex L.*) with an average height of 6 m (Girard et al., 2012; Simioni et al., 2020). Electromagnetic induction and electrical resistivity tomography (ERT) characterized the spatial variability in soil depth (Carrière et al., 2021a).

https://doi.org/10.5194/hess-2024-240
Preprint. Discussion started: 23 September 2024

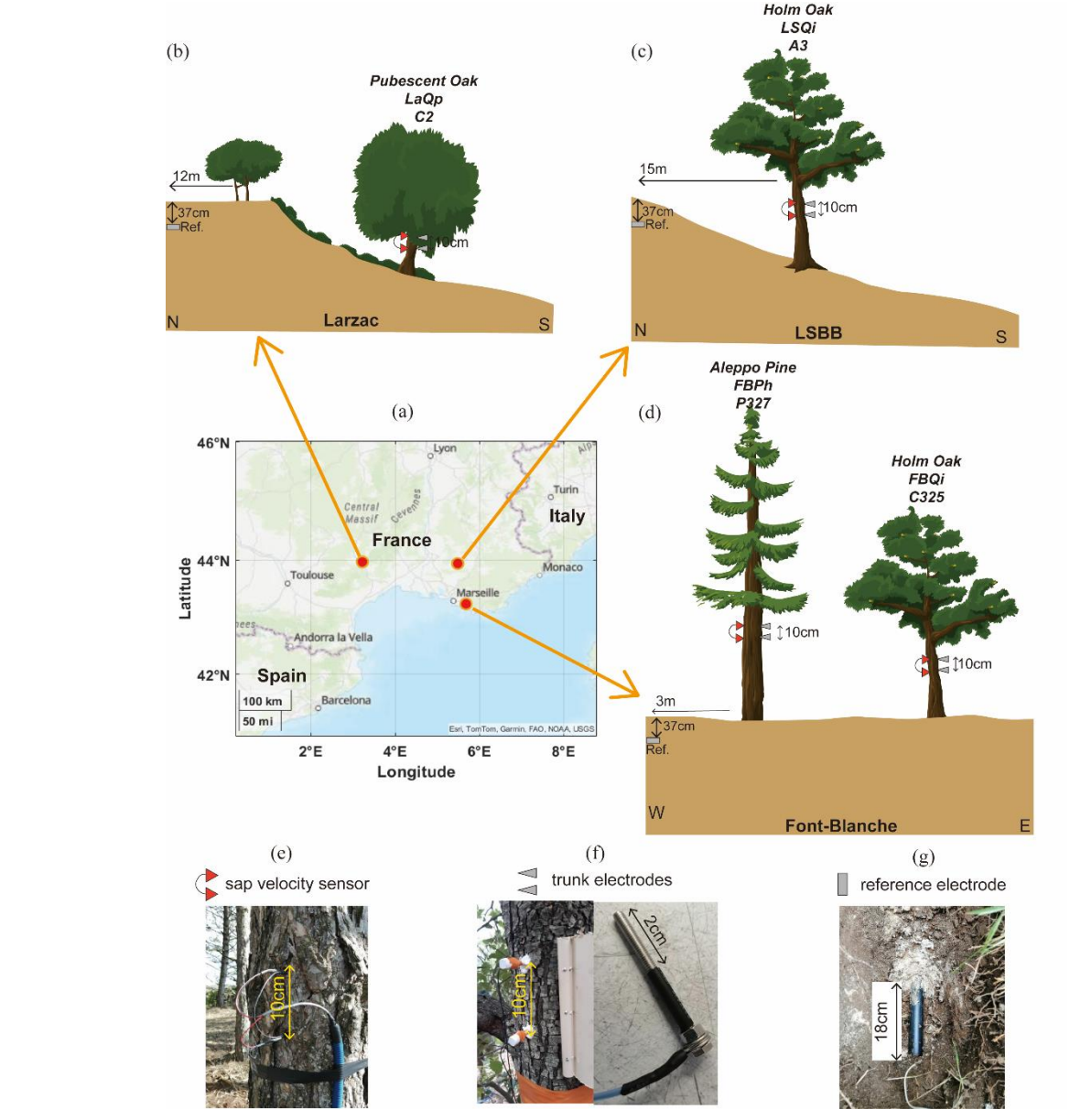

Figure 2: The observation system at the three forest sites: (a) Location map of sites indicated by red circles; (b-d) Observation setups at the Larzac site, the LSBB site, and the Font-Blanche site, respectively; (e-g) Sensors for measuring sap velocity, electrodes for measuring tree SP, reference electrodes buried underground.

The LSBB site, located in the southern part of the Fontaine-de-Vaucluse karst hydrosystem at an altitude of 422 m, is dominated by Holm oak (*Quercus ilex L.*), averaging 13 m in height. The bedrock composition is similar to Font-Blanche. Detailed studies of the site's structure and hydrodynamics were conducted by Carrière et al. (2016) using ERT, ground-penetrating radar, and magnetic resonance sounding. Carrière et al. (2020a, b) examined interindividual drought responses

https://doi.org/10.5194/hess-2024-240
Preprint. Discussion started: 23 September 2024


Hydrology and Earth System Sciences
Discussions

along a transect monitored by ERT. Evapotranspiration at the mountain scale was studied using superconducting gravimetry (Carrière et al., 2021b).

The Larzac observatory, situated at an average altitude of 708 m, features a landscape of grasslands, black pine plantations, and deciduous stands dominated by Pubescent oaks (*Quercus pubescens*), with monitoring focused solely on the oaks. The observatory is part of the Durzon karstic system, primarily composed of dolomite, and has been explored using gravimetry (Fores et al., 2018; Jacob et al., 2008), ERT, and seismic methods (Valois et al., 2016).

Four trees have been equipped with SP and sap velocity sensors (Fig. 2 and Table 1): 1) *Quercus pubescens* at the Larzac observatory with a trunk circumference of 90 cm, 2) *Quercus ilex L.* at the LSBB site with a circumference of 43 cm, and 3) *Pinus halpensis Mill* and *Quercus ilex L.* with circumferences of 108.3 cm and 39.6 cm, respectively, at the Font-Blanche site. These measurements allow us to compare their physiological characteristics of different species under different meteorological and geological conditions.

3.2 Instrument and data

3.2.1 Sap velocity measurements

Data were collected at the three sites throughout 2023 (Table S1 of Supplementary Material). The raw data related to this study can be found in Hu et al. (2024). To assess transpiration rates, sap velocity was measured using the heat dissipation technique by Granier (1987) at the four trees. Two thermocouple probes were inserted 2 cm into the sapwood of each tree, positioned 10 cm apart. The upper probe applied a constant heating power (see Fig. 2e). The temperature difference between the upper and lower probes is influenced by sap flow surrounding the heated probe. The Granier-type heat-dissipation probes were installed at around 1.5 m above the ground of the trees. Thus, by continuously heating in the upper probe, sap velocity could be estimated by measuring the temperature difference between the probe pairs by copper constantan thermocouples under the thermal imbalance. The original signal was recorded in millivolts, subsequently transformed into temperature with a calibration coefficient (~0.04 mV $^{o}C^{-1}$, Do and Rocheteau, 2002). Then, the sap velocity was calculated by the Granier's empirical equation (Granier, 1987) with the obtained temperature differences. After calibration and correction, the sap velocity in $\mu m\ s^{-1}$ at 30-minute intervals (e.g., Moreno et al., 2021).

3.2.2 SP measurements

The electrical voltages were measured using a high-impedance multimeter controlled by a digital data logger. Each tree is equipped with a pair of stainless-steel screws, separated vertically by 10 cm, serving as trunk electrodes. These electrodes were horizontally aligned with the corresponding sap flow sensors on each tree (Fig. 2). After peeling away the bark from the trunk, the electrodes were inserted to a depth of 2 cm to ensure contact with the sapwood. The outside part of the electrodes was coated with black insulating rubber (as depicted in Fig. 2f). All trunk electrodes were identical in material, size, and shape.

https://doi.org/10.5194/hess-2024-240
Preprint. Discussion started: 23 September 2024


Hydrology and Earth System Sciences
Discussions

Following installation, the exposed portions of the electrodes were further shielded with epoxy glue to isolate them from environmental factors and minimize the impact of meteorological conditions such as air temperature, humidity and radiation. Polarizable stainless-steel electrodes were used in previous outdoor experiments for tree SP measurements, such as Gibert et al. (2006) and Zapata et al. (2021). Gibert et al. (2006) discussed the temperature effects of steel electrodes and found that artificially heating and cooling a tree electrode did not result in significant variations in electrical potential compared to another electrode that was not thermally disturbed. In this work, we neglect temperature effects on electrode potentials.

Non-polarizable Petiau-type ($Pb/PbCl_2$) electrodes (Petiau, 2000) were selected as reference electrodes and buried in the soil at a depth of 37 cm (Fig. 2g). The raw signal is a voltage between the trunk and the reference, which includes the electrical potential of tree *in situ* and electrode. In this study, we used the voltage measured at the lower electrode minus the higher electrode to indicate the tree SP.

3.2.3 Meteorological data

The physiological conditions of trees respond to climate changes. We gathered data on actual evapotranspiration (Actual ET), precipitation (Prec.), vapor pressure deficit (VPD), and air temperature (Temp.) from the meteorological station located at the Font-Blanche site. Additionally, a meteorological station near to the LSBB site supplied us with daily precipitation, mean air temperature, and global radiation data. Hourly air temperature and precipitation data were obtained from a meteorological station situated less than 10 km from the Larzac site. Detailed information refers to Table S1 of Supplementary Material.

3.3 Data analysis

3.3.1 Wavelet analysis of sap velocity and tree SP

To identify correlations and phase lags between sap velocity and tree SP at different time scales, we calculated the coherences between the two time-series using continuous wavelet transformation coefficients. The wavelet coherence $C_{SV,SP}(a, b)$ between sap velocity (SV) and SP signals is calculated by:

$$C_{SV,SP}(a, b) = \frac{|S(W_{SV}(a,b)W_{SP}{}^{*}(a,b))|^2}{S(|W_{SV}(a,b)|^2)S(|W_{SP}(a,b)|^2)}, \quad (9)$$

where the superscript * denotes the complex conjugate; S denotes the smoothing operator function (Torrence and Compo, 1998); $W_{SV}(a, b)$ and $W_{SP}(a, b)$ are the continuous wavelet transforms of sap velocity and SP signal at the wavelet scale a and position (frequency or period) b using the Morlet wavelet (e.g., Grinsted et al., 2004; Linde et al., 2011).

3.3.2 Variational mode decomposition

Due to factors such as temperature variations, trunk wounds, and electrode polarization effects, the recorded SP data may exhibit long-period drifts. Additionally, SP measurements are susceptible to high-frequency electromagnetic noise interference. As introduced in Section 2.1, the generation mechanisms of tree SP are complex and multiple. This means that the measured SP in our experimental sites contain signal contributions originating from various sources. Similar to an electrocardiogram

https://doi.org/10.5194/hess-2024-240
Preprint. Discussion started: 23 September 2024


Hydrology and Earth System Sciences
Discussions

(ECG), the tree SP is an electrophysiological signal. The variational mode decomposition (VMD) approach has been applied to process ECG signals and extract the intrinsic modes from signals to obtain information-containing spikes and low-frequency patterns (long-term drifts) related to physiological activities.

VMD can be used to decompose signal $f(t)$ into sub-signals $u_k(t)$ with different center frequencies ω_k (Dragomiretskiy and Zosso, 2014):

$$f(t) = \sum_{k=1}^{N} u_k(t), \tag{10}$$

where *k* and *N* denote the number and total number of decomposed modes. Assuming each mode u_k to be concentrated around a center frequency ω_k in its bandwidth, the below minimization problem is used to determine the decomposition u_k:

$$\min_{\{\omega_k, u_k\}} \left\{ \sum_{k=1}^{N} \left\| \partial_t \left[\left(\delta(t) + \frac{j}{\pi t} \right) * u_k(t) \right] e^{-j\omega_k t} \right\|_2^2 \right\}, \tag{11}$$

where $j^2 = -1$, $\delta(t)$ and $*$ denote the Dirac function and convolution, respectively. More details about the optimization process to solve Eq. (11) with updating the modes and the center frequencies can be found in Dragomiretskiy and Zosso (2014). In this study, we use the frequencies with the center of gravity and the largest amplitudes of the mode's power spectrum to represent the center frequency and the dominant frequency of each corresponding mode, respectively.

4 Results

4.1 Overview of one year of raw data

4.1.1 Raw time-series data

The tree SP data collected at the Font-Blanche site are displayed in Fig. 3 (refer to Section 3.2.2). The time-varying sap velocities and SP obtained on the Aleppo pine trunk (Figs. 3c&e) differ from those of the Holm oak trunk (Figs. 3d&f), even when the two trees are in proximity and experience identical weather conditions (Figs. 2d, 3a&b). Both trees show rather large SP signals with a more pronounced response to environmental changes on Aleppo pine compared to Holm oak. However, the overall time-varying patterns of the raw SP data from trees do not demonstrate a clear correlation with sap velocity, as evidenced by relatively low Pearson correlation coefficients (see Fig. S1 in Supplementary Material). Additional data from the Larzac and LSBB sites are provided in Fig. S2.

https://doi.org/10.5194/hess-2024-240
Preprint. Discussion started: 23 September 2024

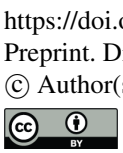

Hydrology and Earth System Sciences
Discussions

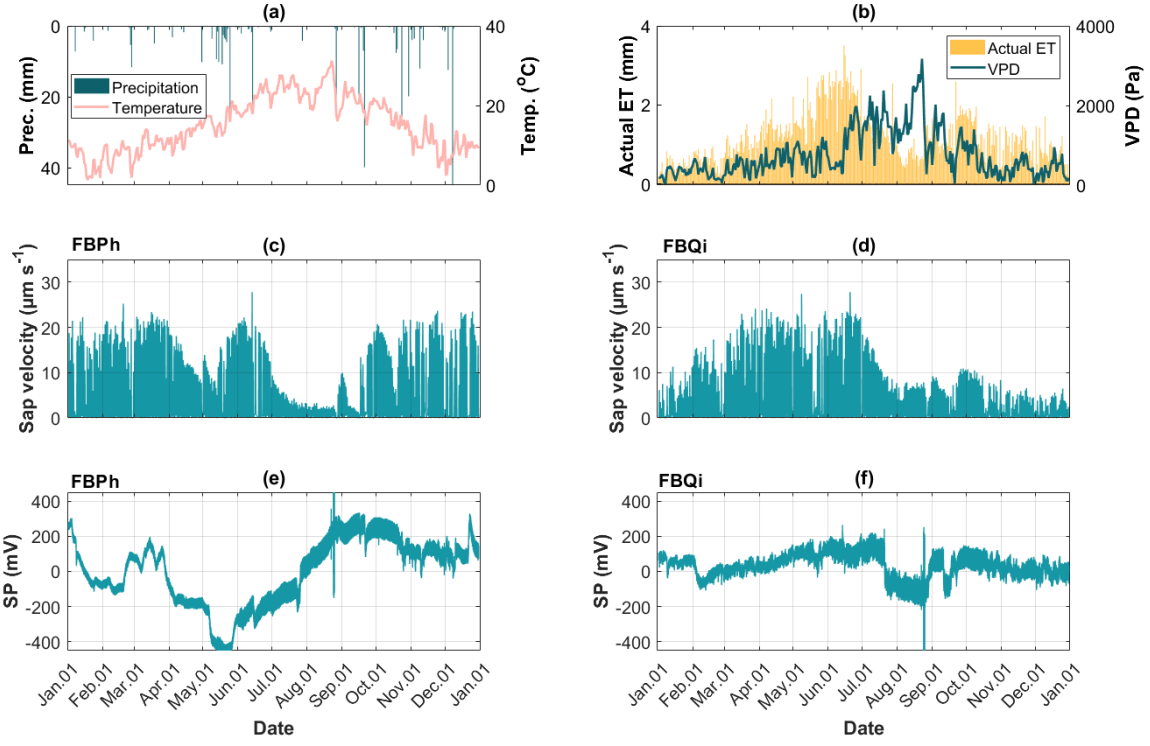

Figure 3: One-year data collected at the Font-Blanche site at half-hourly intervals from January 1, 2023, to January 1, 2024. (a) Precipitation and air temperature data; (b) Actual evapotranspiration (Actual ET) and vapor pressure deficit (VPD) data; (c-d) Sap velocity for the Aleppo pine (FBPh) and the Holm oak (FBQi), respectively; (e-f) SP measurements for the Aleppo pine (FBPh) and the Holm oak (FBQi), respectively.

4.1.2 Wavelet analysis of sap velocity and tree SP

According to Section 3.3.1, we calculated the wavelet coherence between the sap velocity and tree SP data collected throughout 2023. As an example, we present the coherence maps for the two trees at the Font-Blanche site in Fig. 4. The coherence anomalies primarily concentrate around the one-day period, spanning almost the entire year. Notably, tree SP exhibits a negative correlation with sap velocity across the two different species of trees. Note also that the coherence diminishes during periods of water surplus (Fig. 4a). In contrast, the Holm oak at the LSBB site shows lower coherence, and the Pubescent oak at the Larzac site lacks coherence between sap velocity and SP (Fig. S3). The wide discrepancies for different trees at different test sites might be attributed to different annual rainfall (Tabel 1 and Figs. S2a&b) and other factors such as electrochemical and electrode-related effects contributing to the measured SP data.

https://doi.org/10.5194/hess-2024-240
Preprint. Discussion started: 23 September 2024

Hydrology and Earth System Sciences
Discussions

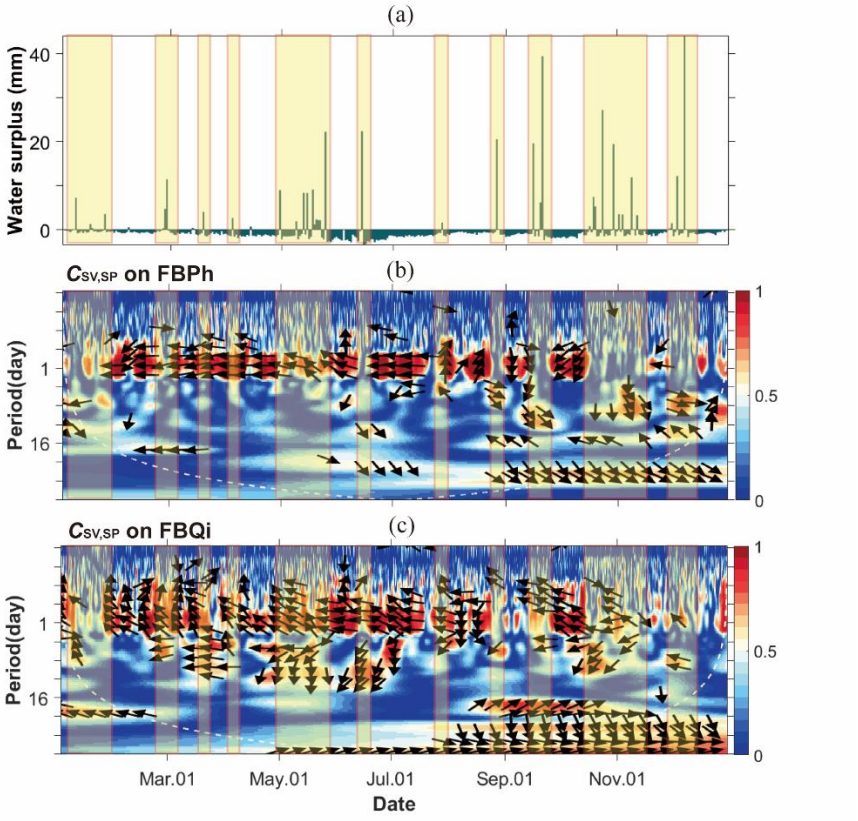

Figure 4: Wavelet coherence analysis between sap velocity and tree SP data at the Font-Blanche site in 2023. (a) Water surplus calculated as the difference between precipitation and actual evapotranspiration; (b-c) Wavelet coherence maps for the Aleppo pine and Holm oak at the Font-Blanche site, respectively, with yellow highlighted boxes indicating periods of water surplus. Arrows denote the lag/lead phase between the two time series; White dashed lines (b-c) indicate the cone of influence where edge artifacts are negligible.

4.2 Decomposition results

In our case, VMD is used to separate the measured data into a finite set of components (modes). We initially assume six principal modes as all coefficients of determination (R^2) between the measured tree SP, sap velocity data with the sum of the corresponding six intrinsic modes using one-year data from 2023 for all four trees are 1.00, meaning that the results of VMD could effectively reconstruct the measurements. As an example, we present the frequency spectra of six modes decomposed from the tree SP and sap velocity (SV) obtained from the Holm oak tree at the Font-Blanche site throughout 2023 (Fig. 5). The center and dominant frequencies of each decomposed mode decrease sequentially. Besides the expected diurnal variations driven by the rhythm of sap flow (Figs. 5i-j), other high-frequency content and low-frequency trends are considered noise and long-term drifts in this study.

https://doi.org/10.5194/hess-2024-240
Preprint. Discussion started: 23 September 2024

Hydrology and Earth System Sciences
Discussions

When compared to the decomposition spectrum of SV data (Figs. 5b&d), noise present in the tree SP data tends to exhibit higher frequencies and proportions (Figs. 5a, c, e, g). The low-frequency trends (baseline) are presented in the last intrinsic modes (Figs. 5k-l). Except for the fifth intrinsic mode, the decompositions of SP and SV exhibit distinctly different frequency characteristics. Notably, the fifth intrinsic modes in both datasets demonstrate a diurnal rhythm, with a dominant frequency of 1 d^{-1} for both SP and SV decompositions (Figs. 5i-j).

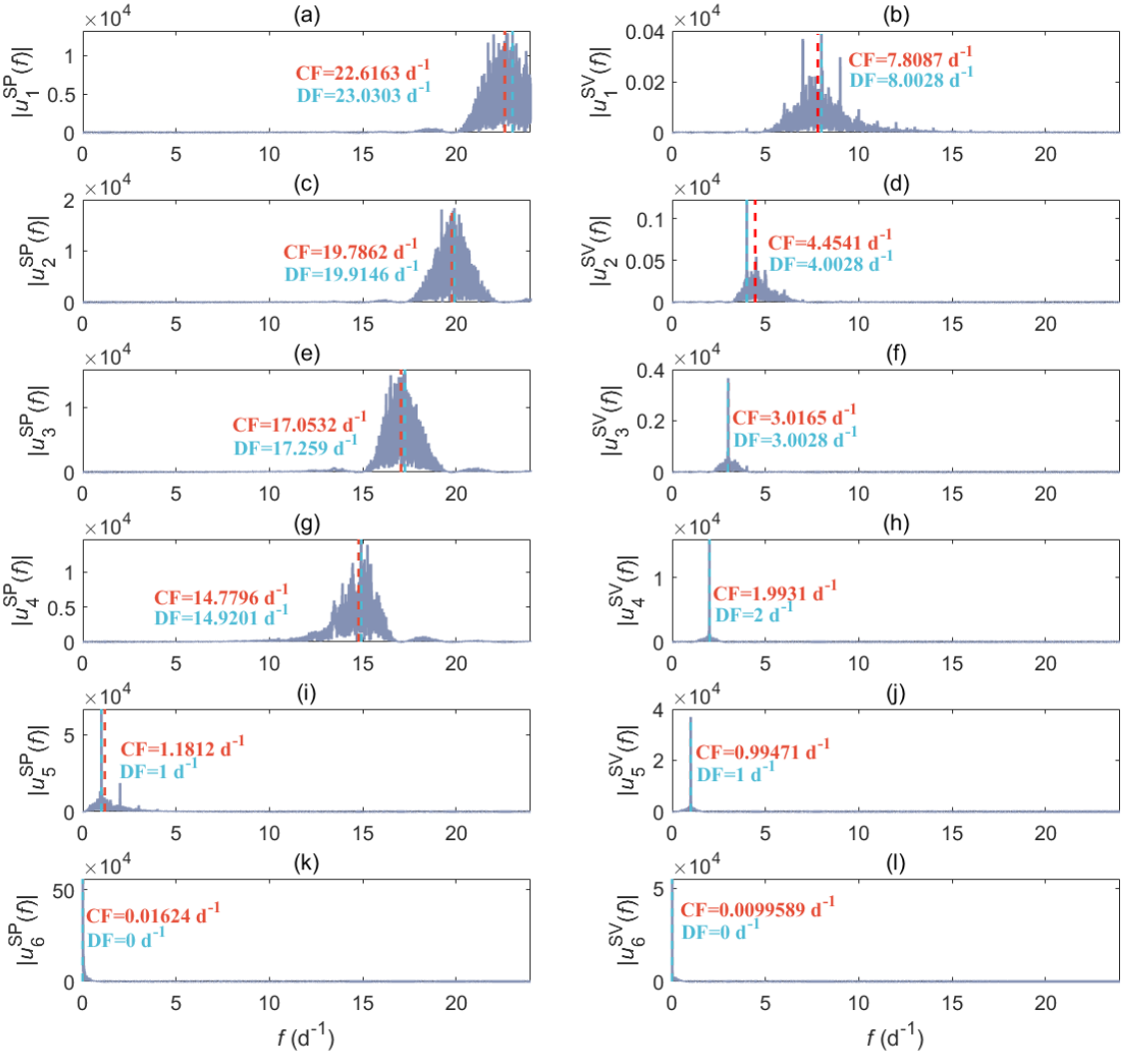

Figure 5: Frequency spectra of six decomposed modes of tree SP (left column: a, c, e, g, i, k) and sap velocity (left column: b, d, f, h, j, l) data obtained on the Holm oak (FBQi) at the Font Blanche site within 2023 using the variational method (VMD); Different rows correspond to different modes, where "CF" and "DF" indicate the center frequency and dominant frequency of the corresponding mode, respectively.

We investigated the impact of increasing the number of modes from 6 to 12 when performing data decomposition. Regardless of the number of modes used, the results consistently indicate a diurnal rhythm in the second last intrinsic mode with similar

https://doi.org/10.5194/hess-2024-240
Preprint. Discussion started: 23 September 2024


Hydrology and Earth System Sciences
Discussions

amplitudes and patterns (refer to Fig. S4). We also conducted an analysis on the tree SP and sap velocity data collected from the neighboring Aleppo pine (FBPh) using the VMD approach (Fig. S5). The frequency bands of each decomposition derived from FBPh are comparable to those from FBQi. Particularly, the high-frequency oscillating characteristics of SP components on both trees are nearly identical. Since our primary interest lies in understanding the diurnal variations associated with transpiration, we employed the same VMD procedure to the whole datasets to extract the fifth decomposed results based on decompositions with six modes.

4.3 The relationship between SP and physiological characteristics of trees

4.3.1 Correlation coefficients between data collected at the Font-Blanche site

Tree transpiration is affected by water availability, VPD, net radiation, and atmospheric uptake of water (e.g., Alfieri et al., 2018). Employing the VMD approach and extracting six intrinsic mode functions, we delineated the diurnal rhythms using the fifth subset component of tree SP, sap velocity and meteorological data collected during a two-week period in the growing season of 2023. The fifth VMD components exhibited significant correlations between tree SP and sap velocity, notably at the Aleppo pine (FBPh) with a correlation coefficient of -0.8516. The cross-correlation coefficients between decomposed sap velocity and SP for the Holm oak (FBQi) trees reached -0.6124. Based on the electrokinetic mechanism generated by sap flow in Section 2.1, a larger negative SP should indicate a higher transpiration rate, which is indicated by the negative signs of the Pearson correlation between the sap velocity and tree SP in this case. Interestingly, the fifth extracted VMD components of tree SP data on FBPh displayed relatively high correlations with other data, including tree SP at FBQi (see Fig. S6). Below, we further analyze the correlations between the time-varying tree SP with the sap velocity data on different trees and sites.

4.3.2 Correlations between tree SP and sap velocity across four trees

To analyze the linear relationship between sap velocity and SP, scatter plots are displayed in Fig. 6 using the fifth VMD modes. The fifth decomposed signals of SP and sap velocity are denoted by "VMD_5^{SP}" and "VMD_5^{SV}", respectively. The fifth VMD results of tree SP and sap velocity data present similar frequency content (Figs. 5i&j). Here, we assume that the fifth VMD results of tree SP originated from diurnal variations of sap velocity. Upon applying linear regression, for two species of trees investigated at the Font-Blanche Forest, the Holm oak (Fig. 6c) exhibits a steeper slope compared to the Aleppo pine (Fig. 6a). Outliers were removed under a 95 % confidence level by the linear regression to obtain the slope coefficients. In contrast, the correlation of decompositions between the tree SP and sap velocity is lower on the Holm oak at the LSBB (Fig. 6e) than on the same species at the Font-Blanche (Fig. 6c). Additionally, there is no correlation found on the Pubescent oak at the Larzac site (Fig. 6g).

https://doi.org/10.5194/hess-2024-240
Preprint. Discussion started: 23 September 2024

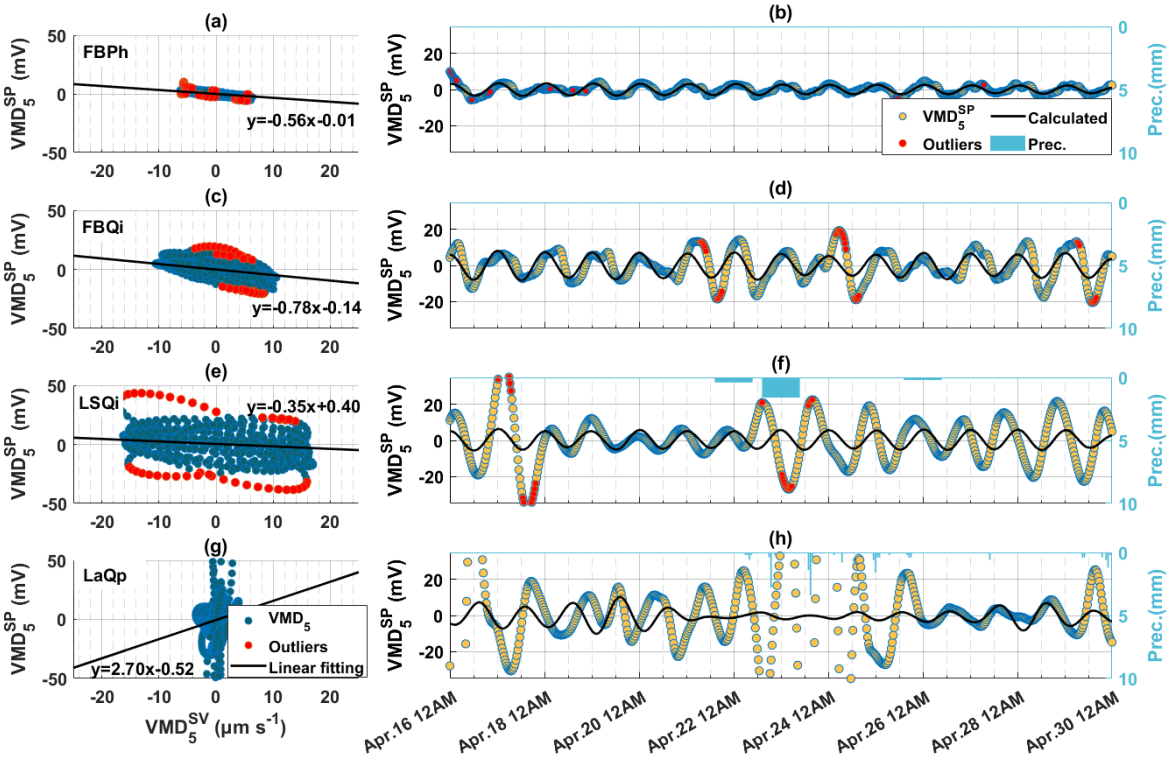

Figure 6: The relationship between the fifth decomposed sap velocity (VMD_5^{SV}) and tree SP data (VMD_5^{SP}) in April 16-30, 2023, at the Font-Blanche, LSBB, and Larzac site. (a, c, e, f) Comparison scatter plots of the decomposed sap velocity and SP data for (a) the Aleppo pine (FBPh), (c) the Holm oak (FBQi) at the Font-Blanche site, (e) the Holm oak at the LSBB (LSQi), and (g) the Pubescent oak at the Larzac (LaQp), with black lines indicating linear regression results and red dots indicating outliers. (b, d, f, h) Corresponding decompositions of SP data (dots) and calculated SP (black lines) based on the linear relationship between VMD_5^{SV} and VMD_5^{SP}, with red dots as outliers from linear regression.

As detailed in Section 3, the height of the lower electrode with respect to the upper electrode on the monitored trunks is -10 cm, allowing us to calculate the electrical potential gradient (∇V) between the measurement points. Moreover, electrical resistivity tomography has been conducted on trunks at both the Font-Blanche and Larzac sites. The average sapwood resistivities of the Aleppo Pine and the Holm oak at the Font-Blanche are 369 Ω·m and 250 Ω·m, respectively (e.g., Moreno et al., 2021). By converting the SP and sap velocity data to the International System of Units, we estimated the effective excess charge density ($\hat{Q}_v = \frac{\sigma \nabla V}{\mathbf{u}}\Big|_{\mathbf{J=0}}$) using linear fitting slope coefficients $\left(\frac{\nabla V}{\mathbf{u}}\right)$. The resulting $\hat{Q}_v$ values for FBPh and FBQi are 15.2 C m^{-3} and 31.2 C m^{-3}, respectively, consistent with those typically found in porous media (pH ranging from 6 to 8.5), such as sandstones, glass beads, and limestones (Jardani et al., 2007; Revil and Jardani, 2013). These materials correspond to typical pore sizes of 10 - 100 μm, which is of the same order of magnitude as the diameter of the cells conducting the sap (e.g., Sperry, 2003).

Using the parameters obtained from the linear regression (Figs. 6a, c, e, g), we predicted the tree SP responses as a function of the sap velocity (refer to Figs. 6b, d, f, h). The predictions effectively replicate the time-varying SP patterns observed in the

https://doi.org/10.5194/hess-2024-240
Preprint. Discussion started: 23 September 2024

Hydrology and Earth System Sciences
Discussions

Aleppo pine at the Font-Blanche (Fig. 6b). Rainfall events decreased the coherence and increased the phase shifts between sap velocity and tree SP (Fig. 4). In this case, due to the rainfall events during the extracted period at both LSBB and Larzac sites, the VMD_5^{SV} could not restore the VMD_5^{SP} obtained from the measured data (Figs. 6f&h). Additionally, the modeled tree SP for the Holm oak at the Font-Blanche fails to accurately capture the highly varying amplitudes observed in the measured SP data (Fig. 6d). Specifically, elevated SP amplitudes are noted on April 22 and 24.

To test if the VMD decomposition of sap velocity data decreases the original amplitude when removing other components, we compared the raw SP and sap velocity data with the sum of the diurnal features (VMD_5^{SP}, VMD_5^{SV}) and the baseline (VMD_6^{SP}, VMD_6^{SV}) in data processed by the VMD approach (Fig. 7). The highest diurnal magnitudes of the raw and the processed sap velocity data are relatively stable compared with the tree SP data, and no clear increasing characteristics are shown on April 22 and 24. Thus, even when using all decompositions except the last mode (baseline) of sap velocity data to estimate the diurnal tree SP based on their linear relationship, the higher SP magnitudes on April 22 and 24 cannot be reconstructed (Fig. 7c). In addition, we obtained similar results when we used a finite impulse response filter to process the data (Fig. 7d). This test indicates that the higher SP magnitudes might be induced by factors other than sap velocity.

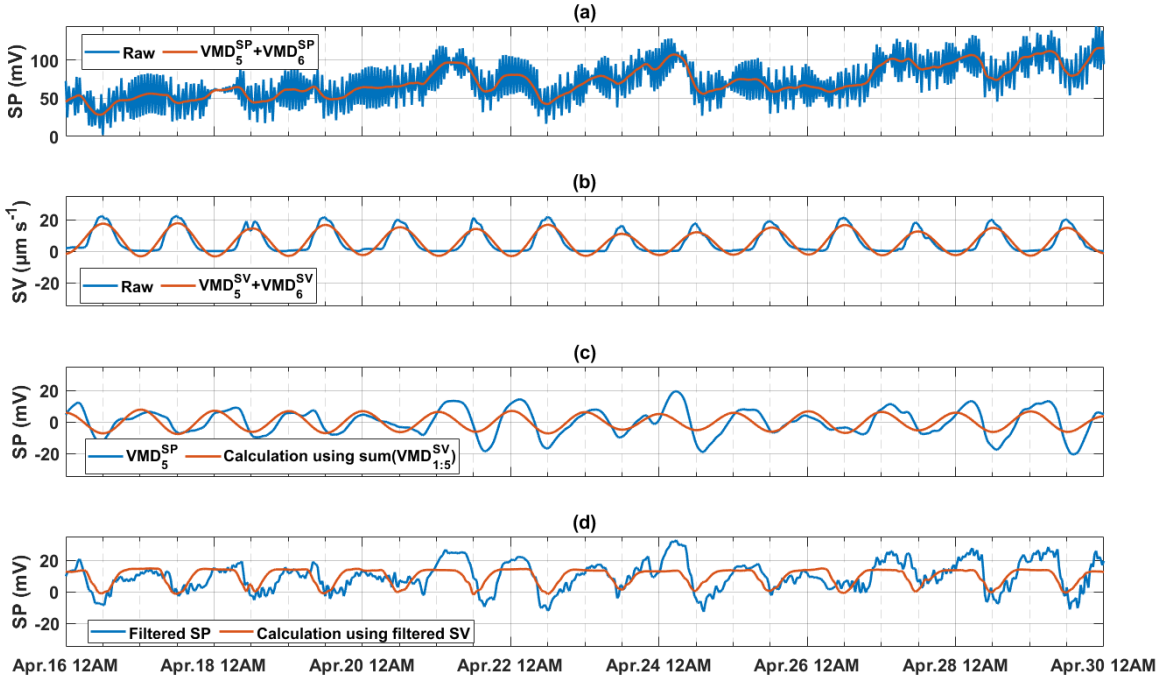

Figure 7: The two-week SP data during the 2023 growing season for the Holm oak (FBQi) at the Font-Blanche site processed using different approaches. (a) Raw SP data and the sum of the last two SP decompositions using VMD; (b) Raw sap velocity data and the sum of the last two sap velocity decompositions using VMD; (c) Fifth SP decomposition using VMD and calculated SP using the sum of the first to fifth sap velocity decompositions by VMD; (d) Filtered SP data using a finite impulse response filter (bandpass: 1/48 h^{-1} to 1/1.5 h^{-1}; filter order: 100) and calculated SP using filtered sap velocity data with the same filter parameters.

https://doi.org/10.5194/hess-2024-240
Preprint. Discussion started: 23 September 2024


Hydrology and Earth System Sciences
Discussions

5 Discussion

5.1 Hydraulic properties and tree SP

The distinctly different woody anatomy of pine and oak trees contributes to differences in their hydraulic properties and water storage capacities within the stem (Butterfield, 2003; Steppe and Lemeur, 2007). Increases in water content leads to increases in the electrical conductivity of the stem, potentially decreasing the electrical voltages (Eq. 5). Assuming the xylem conduits behave similarly to porous materials, the empirical relationship between the hydraulic permeability k and $\hat{Q}_v$ for porous materials is expressed by (Jardani et al., 2007):

$$\log_{10}(\hat{Q}_v) = -9.23 - 0.82\log_{10}k. \quad (12)$$

It is seen that increasing permeability leads to a decreasing effective excess charge density, subsequently reducing electrical streaming current density (Eq. 3) and weakening the electrokinetic effect. If water dynamics in vascular plants are similar to water flow in a vadose zone, as the water content increases, the effective permeability increases while the effective excess charge density decreases. Thus, when we observe increases in water content, we cannot distinguish whether decreases in tree SP were caused by weakening electrokinetic effect or increasing electrical conductivity. This lack of identifiability often occurs in SP interpretation of water dynamics in the critical zone (e.g., Hu et al., 2020). Conducting time-lapse electrical resistivity tomography on the trunk (e.g., Harmon et al., 2021) might help to separate the variables affecting the ratios of the tree SP to the sap velocity.

Referring to Eq. (12) and the results in Section 4.3.2, we estimate the permeabilities of sapwood to be 2.01×10^{-13} m^2 for the Aleppo pine at the Font-Blanche site and 8.35×10^{-14} m^2 for the Holm oak at the same site in late April of 2023. Ionic content and pH of xylem sap are reported to contribute to differences in hydraulic properties (López-Portillo et al., 2005; Losso et al., 2023). Referring to Eqs. (2)-(4) of Section 2.1 and assuming the electrical conductivity of xylem sap σ_f is 270 µS cm^{-1} (Losso et al., 2023), and the dielectric permittivity of xylem sap ϵ_f is 7.10×10^{-10} F m^{-1} (water at 20 °C), the corresponding Zeta potentials are estimated to be -42.87 mV for FBPh and -24.77 mV for FBQi, respectively. These Zeta potentials are of similar magnitude as typical values at the surface of silica grains in contact with an electrolyte, with concentration in the range of several millimoles per liter of NaCl (Revil et al., 1999). Although a lower sap rate is observed, a stronger electrokinetic coupling capacity in a tree still induces a larger amplitude SP. This suggests that the electrokinetic effects generated by sap flow might have similar characteristics to porous media. Thus, it has potential for short-term predictions using tree SP to evaluate sap velocity.

As discussed in Section 2.1, several factors affect or alter tree SP. However, we contend that the gravitational forces driven by lunar-solar tides do not dominate tree SP generation as suggested in previous studies (Barlow 2012; Le Mouël et al., 2024). First, rainfall events do not change gravitational forces, yet tree SP was clearly affected by rainfall (e.g., Figs. 6f&h). Second, a strong link between diurnal tree SP and sap velocity is observed during the growing season, independent of rainfall (e.g., Figs. 4, 6a&b). While sap flow may not be the sole mechanism for tree SP generation, our results suggest a close relationship

https://doi.org/10.5194/hess-2024-240
Preprint. Discussion started: 23 September 2024


Hydrology and Earth System Sciences
Discussions

between tree SP and sap velocity. Further studies with monitoring of electrical resistivity, solute concentration, and water content in sapwood are needed to elucidate the mechanisms behind tree SP generation and variation.

5.2 Electrochemical effects

The results presented in Sections 4.3 indicate that the electrokinetic mechanism fails to fully explain the amplitudes of tree SP and the phase shifts between the diurnal variations of the measured SP and predicted SP from measured sap velocity data. Researchers propose that pH gradients contribute to SP differences (e.g., Gil and Vargas, 2023; Love et al., 2008;). According to the Nernst potential:

$$\varphi_{\mathrm{pH}}^{\mathrm{lower}} - \varphi_{\mathrm{pH}}^{\mathrm{upper}} = -\frac{k_{\mathrm{B}} T_{\mathrm{K}}}{\mathrm{e}_0 q_i}(\mathrm{pH}^{\mathrm{lower}} - \mathrm{pH}^{\mathrm{upper}}), \quad (13)$$

a higher pH value at the position of the upper electrode leads to a downward gradient of the electrical potential.

Schill et al. (1996) observed a decreasing trend in pH value and an increasing trend in osmotic potential in the xylem sap of two maple trees with increasing height above ground. The rate of decrease in pH is higher in the lower part of trunk, with values ranging from 6.6 to 7.4 and a rate of approximately 0.8 m^{-1} (Schill et al., 1996). Assuming a pH difference of 0.1 over 10 cm, the induced electrical potential difference would be -2.53 mV at 293.15 K (20 °C), given that k_B is the Boltzmann constant and e_0 is the elementary charge. Consequently, under an upward sap flow, a positive pH difference leads to a more negative SP difference between the lower and upper electrodes. This factor may contribute to the underestimation of SP when utilizing the VMD-based sap velocity component (e.g., Figs. 6d, f, h).

In addition to the ion H^+ transport, previous experiments have observed upward longitudinal concentration gradients of metal ions (K^+, Ca^{2+}, Mg^{2+}) on tree stems, although this phenomenon is not occurring for all trees (McDonald et al., 2002). Therefore, the actual sap chemical environment of the investigated tree may involve complex coupling processes, resulting in a relationship between tree SP and sap velocity that does not follow a strict linear model.

5.3 Experimental set-up concerning tree SP

The relationship between SP and upward sap flow does not systematically show a linear pattern. To explore the spatial characteristics associated with physiological processes, further observations are required, particularly regarding measurements at different heights and radial positions along the growing direction. Moreover, comprehending the chemical environment surrounding the electrodes can elucidate electrochemical potential differences, aiding in the explanation of amplitudes and polarization effects (e.g., Jougnot and Linde, 2013).

In our measurements, stainless steel electrodes were employed to measure trunk SP. Compared to other materials such as copper or aluminum, stainless steel electrodes demonstrate relatively stable performance (Hao et al., 2015). However, it's essential to note that metal electrodes are sensitive to environmental changes and have a risk to be polarized. Although the distance between the tree electrodes is small, monitoring the temperature and adding two or three electrodes around each

https://doi.org/10.5194/hess-2024-240
Preprint. Discussion started: 23 September 2024


Hydrology and Earth System Sciences
Discussions

measured point can allow corrections for electrode drift induced by electrode-related effects, enabling a more accurate determination of the tree SP related to physiological changes.

As outlined earlier, all analyses conducted in Section 4 were performed without considering electrode effects. In future research, we suggest an improved experimental setup that involves distributing electrodes along the trunk with greater spacing (e.g., Fig. S7) and using duplicated measurements to ensure that the conclusions are robust. By enhancing the experimental setup, we will further strengthen our current understanding regarding the relationship between tree SP and the transpiration process.

Furthermore, our current observations suggest the presence of other effects in physiological processes. We recommend utilizing ion-selective electrodes to assess the contributions of different ions to SP observations. An experimental setup, coupled with ionic content measurements, and combined with physiochemical modeling, may further enhance understanding of tree SP.

6 Conclusions

By conducting SP and sap velocity measurements on three tree species in the Mediterranean region, we observed high coherence between tree SP and sap velocity at diurnal time scales over a one-year dataset. This coherence diminished and phase shifts increased on days with higher water supply. Our results indicate that different tree species at the same site exhibit different SP patterns. Specifically, two Holm oak trees demonstrated SP characteristics that depend on weather conditions, particularly precipitation, and exhibited different ratios of diurnal SP to sap velocity.

Assuming the electrokinetic mechanism as the primary electrophysiological effect, we estimated the excess charge densities and Zeta potentials of Holm oak and Aleppo pine at the same site using a linear regression model. The values obtained fell within the typical range for porous rock materials. Unlike point measurements of sap velocity, SP signals reflect an integrated bioelectrical process between the two electrodes, but are also influenced by electrode-related effects and environmental factors. The electrokinetic effect predominantly influences tree SP during the dry growing season, suggesting its potential application in evaluating transpiration rates.

This study monitored tree SP at short separations and using only one electrode pair for each tree. Developing better electrode materials, experimental designs and incorporating physiochemical modeling are essential for a deeper understanding of the complex bioelectrical potentials of trees related to transpiration. Additionally, other coupling effects, such as the electro-diffusive mechanism and non-uniform sap flow, also contribute to variations in tree SP, which should be considered in modeling and interpretation of SP.

https://doi.org/10.5194/hess-2024-240
Preprint. Discussion started: 23 September 2024

CRediT authorship contribution statement

Kaiyan Hu: Conceptualization, Methodology, Fornal analysis, Data curation, Writing- Original Draft, Writing - Review & Editing, Visualization.

Bertille Loiseau: Investigation, Data curation, Writing - Review & Editing.

Simon D. Carrière: Investigation, Writing- Original Draft, Writing - Review & Editing.

Nolwenn Lesparre: Conceptualization, Writing - Review & Editing.

Cédric Champollion: Investigation, Writing - Review & Editing.

Nicolas K. Martin-StPaul: Supervision, Data curation.

Niklas Linde: Conceptualization, Methodology, Writing- Original Draft, Writing - Review & Editing, Supervision.

Damien Jougnot: Conceptualization, Methodology, Writing- Original Draft, Writing - Review & Editing, Project administration, Supervision.

Declaration of competing interests

The authors declare that they have no known competing financial interests or personal relationships that could have appeared to influence the work reported in this paper.

Data availability

All data used in this study are available in the hydrogeophysics community of Zenodo (https://doi.org/10.5281/zenodo.12662288) and will also be published on the H+ National Observatory Service with free access.

Acknowledgements

The authors acknowledge the financial support of OZCAR Research Infrastructure, the H+ National Observatory Service and OSU OREME for funding part of this work. Nolwenn Lesparre, Damien Jougnot, and Simon Carrière also thank the MOOSE project, an EC2CO initiative. Kaiyan Hu thanks the financial support by the Postdoctoral Fellowship Program of China Postdoctoral Science Foundation (GZC20241598, 2024M753016) and the "CUG Scholar" Scientific Research Funds at China University of Geosciences (Wuhan) (Project No. 2023139).

References

Al Mahrouqi, D., Vinogradov, J., and Jackson, M. D., Zeta potential of artificial and natural calcite in aqueous solution, Adv. Colloid Interface Sci., 240, 60-76, doi:10.1016/j.cis.2016.12.006, 2017.

https://doi.org/10.5194/hess-2024-240
Preprint. Discussion started: 23 September 2024

Alfieri, J. G., Kustas, W. P., and Anderson, M. C.: A brief overview of approaches for measuring evapotranspiration, Agroclimatology: Linking Agriculture to Climate, 60, 109-127, https://doi.org/10.2134/agronmonogr60.2016.0034, 2018.

Anderegg, W. R., Klein, T., Bartlett, M., Sack, L., Pellegrini, A. F., Choat, B., and Jansen, S.: Meta-analysis reveals that hydraulic traits explain cross-species patterns of drought-induced tree mortality across the globe, Proc. Natl. Acad. Sci. U.S.A., 113(18), 5024-5029, https://doi.org/10.1073/pnas.1525678113, 2016.

Bachofen, C., Poyatos, R., Flo, V., Martínez-Vilalta, J., Mencuccini, M., Granda, V., and Grossiord, C.: Stand structure of Central European forests matters more than climate for transpiration sensitivity to VPD, J. Appl. Ecol., 60(5), 886-897, https://doi.org/10.1111/1365-2664.14383, 2023.

Barlow, P. W.: Moon and cosmos: plant growth and plant bioelectricity, in: Plant Electrophysiology: Signaling and Responses, edited by: Volkov, A. G., Springer, Berlin, Heidelberg, Germany, 249-280, https://doi.org/10.1007/978-3-642-29110-4_10, 2012.

Belashev, B.: Monitoring the electrical potential difference of pine tree, BIO Web Conf., 93, 01015, https://doi.org/10.1051/bioconf/20249301015, 2024.

Butterfield, B. G.: Wood anatomy in relation to wood quality, Wood Quality and Its Biological Basis, 683, 30-52, 2003.

Carriere, S., Chalikakis, K., Danquigny, C., Davi, H., Mazzilli, N., Ollivier, C., Emblanch, C.: The role of porous matrix in water flow regulation within a karst unsaturated zone: an integrated hydrogeophysical approach, Hydrogeol. J., 24(7), 1905-1918, https://doi.org/10.1007/s10040-016-1425-8, 2016.

Carrière, S. D., Ruffault, J., Pimont, F., Doussan, C., Simioni, G., Chalikakis, K., ... and Martin-StPaul, N. K.: Impact of local soil and subsoil conditions on inter-individual variations in tree responses to drought: insights from Electrical Resistivity Tomography, Sci. Total Environ., 698, 134247, https://doi.org/10.1016/j.scitotenv.2019.134247, 2020a.

Carrière, S. D., Ruffault, J., Cakpo, C. B., Olioso, A., Doussan, C., Simioni, G., ... and MartinSt-Paul, N. K.: Intra-specific variability in deep water extraction between trees growing on a Mediterranean karst, J. Hydrol., 590, 125428, https://doi.org/10.1016/j.jhydrol.2020.125428, 2020b.

Carrière, S. D., Martin-StPaul, N. K., Doussan, C., Courbet, F., Davi, H., and Simioni, G.: Electromagnetic induction is a fast and non-destructive approach to estimate the influence of subsurface heterogeneity on forest canopy structure, Water, 13(22), 3218, https://doi.org/10.3390/w13223218, 2021a.

Carrière, S. D., Loiseau, B., Champollion, C., Ollivier, C., Martin-StPaul, N. K., Lesparre, N., ... and Jougnot, D.: First evidence of correlation between evapotranspiration and gravity at a daily time scale from two vertically spaced superconducting gravimeters, Geophys. Res. Lett., 48(24), e2021GL096579, https://doi.org/10.1029/2021GL096579, 2021b.

Davies, E.: Electrical Signals in Plants: Facts and Hypotheses, in: Plant Electrophysiology: Theory and Methods, edited by Volkov, A. G., Springer, Berlin, Heidelberg, Germany, 407-422, https://doi.org/10.1007/978-3-540-37843-3_17, 2006.

Do, F., and Rocheteau, A.: Influence of natural temperature gradients on measurements of xylem sap flow with thermal dissipation probes. 1. Field observations and possible remedies, Tree Physio L., 22(9), 641-648, https://doi.org/10.1093/treephys/22.9.641, 2002.

Dragomiretskiy, K., and Zosso, D.: Variational mode decomposition, IEEE Trans. Signal Process., 62(3), 531-544, https://doi.org/10.1109/TSP.2013.2288675, 2014.

Dumont, M., and Singha, K.: Geophysics as a hypothesis-testing tool for critical zone hydrogeology, Wiley Interdisciplinary Reviews: Water, e1732, https://doi.org/10.1002/wat2.1732, 2024.

Fensom, D. S.: The bio-electric potentials of plants and their functional significance: I. An electrokinetic theory of transport, Can. J. Bot., 35(4), 573-582, https://doi.org/10.1139/b57-047, 1957.

Fensom, D. S.: The bioelectric potentials of plants and their functional significance: V. Some daily and seasonal changes in the electrical potential and resistance of living trees, Can. J. Bot, 41(6), 831-851, https://doi.org/10.1139/b63-068, 1963.

Fisher, J. B., Melton, F., Middleton, E., Hain, C., Anderson, M., Allen, R., ... and Wood, E. F.: The future of evapotranspiration: Global requirements for ecosystem functioning, carbon and climate feedbacks, agricultural management, and water resources, Water Resour. Res., 53(4), 2618-2626, https://doi.org/10.1002/2016WR020175, 2017.

Flo, V., Martinez-Vilalta, J., Steppe, K., Schuldt, B., and Poyatos, R.: A synthesis of bias and uncertainty in sap flow methods, Agric. For. Meteorol., 271, 362-374, https://doi.org/10.1016/j.agrformet.2019.03.012, 2019.

Fores, B., Champollion, C., Mainsant, G., Albaric, J., and Fort, A.: Monitoring saturation changes with ambient seismic noise and gravimetry in a karst environment, Vadose Zone J., 17(1), 1-12, https://doi.org/10.2136/vzj2017.09.0163, 2018.

Fromm, J., and Lautner, S. Electrical signals and their physiological significance in plants, Plant Cell Environ., 30(3), 249-257, https://doi.org/10.1111/j.1365-3040.2006.01614.x, 2007.

Fromm, J., and Lautner, S.: Generation, transmission, and physiological effects of electrical signals in plants, in: Plant Electrophysiology: Signaling and Responses, edited by Volkov, A. G., Springer, Berlin, Heidelberg, Germany, 207-232, https://doi.org/10.1007/978-3-642-29110-4_8, 2012.

Gaillardet, J., Braud, I., Hankard, F., Anquetin, S., Bour, O., Dorfliger, N., ... and Zitouna, R. OZCAR: The French network of critical zone observatories, Vadose Zone J., 17(1), 1-24, https://doi.org/10.2136/vzj2018.04.0067, 2018.

Gibert, D., Le Mouël, J. L., Lambs, L., Nicollin, F., and Perrier, F.: Sap flow and daily electric potential variations in a tree trunk, Plant Sci., 171(5), 572-584, https://doi.org/10.1016/j.plantsci.2006.06.012, 2006.

Gielen, B., de Beeck, M. O., Loustau, D., Ceulemans, R., Jordan, A., and Papale, D.: Integrated carbon observation system (icos): An infrastructure to monitor the european greenhouse gas balance, in: Terrestrial Ecosystem Research Infrastructures, CRC Press, 505-520, 2017.

Gil, P., and Vargas, A. I.: Stem electrical potential variations may aid in the early detection of drought stress in fruit-bearing trees, Int. J. Agric. Nat. Resour., 50(3), 116-129, https://doi.org/10.7764/ijanr.v50i3.2552, 2023.

Gindl, W., Löppert, H. G., and Wimmer, R. Relationship between streaming potential and sap velocity in *Salix Alba L*, Phyton-Annales Rei Botanicae, 39(2), 217-224, 1999.

585 Girard, F., Vennetier, M., Guibal, F., Corona, C., Ouarmim, S., and Herrero, A.: *Pinus halepensis Mill*. crown development and fruiting declined with repeated drought in Mediterranean France, Eur. J. For. Res., 131, 919-931, https://doi.org/10.1007/s10342-011-0565-6, 2012.

Granier, A.: Evaluation of transpiration in a Douglas-fir stand by means of sap flow measurements, Tree Physiol., 3(4), 309-320, 1987.

590 Grinsted, A., Moore, J. C., and Jevrejeva, S.: Application of the cross wavelet transform and wavelet coherence to geophysical time series, Nonlinear Process. Geophys., 11(5/6), 561-566, https://doi.org/10.5194/npg-11-561-2004, 2004.

Hao, Z., Wang, G., Li, W., Zhang, J., and Kan, J.: Effects of electrode material on the voltage of a tree-based energy generator, PLoS One, 10(8), e0136639, https://doi.org/10.1371/journal.pone.0136639, 2015.

Harmon, R. E., Barnard, H. R., Day-Lewis, F. D., Mao, D., and Singha K.: Exploring environmental factors that drive diel
595 variations in tree water storage using wavelet analysis, Front. Water, 3, 682285, https://doi.org/10.3389/frwa.2021.682285, 2021.

Hermans, T., Goderniaux, P., Jougnot, D., Fleckenstein, J. H., Brunner, P., Nguyen, F., Linde, N., Huisman, J. A., Bour, O., Lopez Alvis, J., Hoffmann, R., Palacios, A., Cooke, A.-K., Pardo-Álvarez, Á., Blazevic, L., Pouladi, B., Haruzi, P., Fernandez Visentini, A., Nogueira, G. E. H., Tirado-Conde, J., Looms, M. C., Kenshilikova, M., Davy, P., and Le Borgne, T.: Advancing
600 measurements and representations of subsurface heterogeneity and dynamic processes: towards 4D hydrogeology, Hydrol. Earth Syst. Sci., 27, 255–287, https://doi.org/10.5194/hess-27-255-2023, 2023.

Hedrich, R., and Schroeder, J. I.: The physiology of ion channels and electrogenic pumps in higher plants, Annu. Rev. Plant Biol., 40(1), 539-569, https://doi.org/10.1146/annurev.pp.40.060189.002543, 1989.

Hölttä, T., Vesala, T., Sevanto, S., Perämäki, M., and Nikinmaa, E.: Modeling xylem and phloem water flows in trees according
605 to cohesion theory and Münch hypothesis, Trees, 20, 67-78, https://doi.org/10.1007/s00468-005-0014-6, 2006.

Hu, K., Jougnot, D., Huang, Q., Looms, M. C., and Linde, N.: Advancing quantitative understanding of self-potential signatures in the critical zone through long-term monitoring, J. Hydrol., 585, 124771, https://doi.org/10.1016/j.jhydrol.2020.124771, 2020.

Hu, K., Loiseau, B., Carrière, S., Lesparre, N., Champollion, C., Martin-StPaul, N., Linde, N., and Jougnot, D.: Dataset for
610 "Self-potential signals related to tree transpiration in a Mediterranean climate" [data set], Zenodo, https://doi.org/10.5281/zenodo.12662288, 2024.

Hubbard, C. G., West, L. J., Morris, K., Kulessa, B., Brookshaw, D., Lloyd, J. R., and Shaw, S.: In search of experimental evidence for the biogeobattery, J. Geophys. Res. Biogeosci., 116, G04018, https://doi.org/10.1029/2011JG001713, 2011.

Islam, M., Janssen, D., Chao, D., Gu, J., Eisen, D., and Choa, F.: Electricity derived from plants, Journal of Energy and Power
615 Engineering, 11(9), 614-619, https://doi.org/10.17265/1934-8975/2017.09.007, 2017.

Jacob, T., Bayer, R., Chery, J., Jourde, H., Le Moigne, N., Boy, J. P., ... and Brunet, P.: Absolute gravity monitoring of water storage variation in a karst aquifer on the Larzac plateau (Southern France), J. Hydrol., 359(1-2), 105-117, https://doi.org/10.1016/j.jhydrol.2008.06.020, 2008.

Jardani, A., Revil, A., Boleve, A., Crespy, A., Dupont, J. P., Barrash, W., and Malama, B.: Tomography of the Darcy velocity from self-potential measurements, Geophy. Res. Lett., 34(24), https://doi.org/10.1029/2007GL031907, 2007.

Jasechko, S., Sharp, Z. D., Gibson, J. J., Birks, S. J., Yi, Y., and Fawcett, P. J.: Terrestrial water fluxes dominated by transpiration. Nature, 496(7445), 347-350, https://doi.org/10.1038/nature11983, 2013.

Jayawickreme, D. H., Jobbágy, E. G., and Jackson, R. B.: Geophysical subsurface imaging for ecological applications, New Phytol., 201(4), 1170-1175, https://doi.org/10.1111/nph.12619, 2014.

Jougnot, D., Linde, N., Revil, A., and Doussan, C. Derivation of soil-specific streaming potential electrical parameters from hydrodynamic characteristics of partially saturated soils, Vadose Zone J., 11(1), https://doi.org/10.2136/vzj2011.0086, 2012.

Jougnot, D., and Linde, N.: Self-potentials in partially saturated media: The importance of explicit modeling of electrode effects, Vadose Zone J., 12(2), 1-21, https://doi.org/10.2136/vzj2012.0169, 2013.

Jougnot, D., Linde, N., Haarder, E. B., and Looms, M. C.: Monitoring of saline tracer movement with vertically distributed self-potential measurements at the HOBE agricultural test site, Voulund, Denmark, J. Hydrol., 521, 314-327, https://doi.org/10.1016/j.jhydrol.2014.11.041, 2015.

Jougnot, D., Mendieta, A., Leroy, P., and Maineult, A.: Exploring the effect of the pore size distribution on the streaming potential generation in saturated porous media, insight from pore network simulations, J. Geophys. Res. Solid Earth, 124(6), 5315-5335, https://doi.org/10.1029/2018JB017240, 2019.

Jougnot, D., Roubinet, D., Guarracino, L., and Maineult, A.: Modeling Streaming Potential in Porous and Fractured Media, Description and Benefits of the Effective Excess Charge Density Approach, in: Advances in Modeling and Interpretation in Near Surface Geophysics, edited by Biswas, A., and Sharma, S., Springer, Cham, Switzerland, 61-96, https://doi.org/10.1007/978-3-030-28909-6_4, 2020.

Köcher, P., Horna, V., and Leuschner, C.: Stem water storage in five coexisting temperate broad-leaved tree species: significance, temporal dynamics and dependence on tree functional traits, Tree Physiol., 33(8), 817-832, https://doi.org/10.1093/treephys/tpt055, 2013.

Koppán, A., Fenyvesi, A., Szarka, L., and Westergom, V.: Measurement of electric potential difference on trees, Acta Biol. Szeged., 46(3-4), 37-38, https://abs.bibl.u-szeged.hu/index.php/abs/article/view/2232, 2002.

Kormiltsev, V. V., Ratushnyak, A. N., and Shapiro, V. A.: Three-dimensional modeling of electric and magnetic fields induced by the fluid flow movement in porous media, Phys. Earth Planet. Inter., 105(3), 109–118, https://doi.org/10.1016/S0031-9201(97)00116-7, 1998.

Kuang, X., Liu, J., Scanlon, B. R., Jiao, J. J., Jasechko, S., Lancia, M., ... and Zheng, C.: The changing nature of groundwater in the global water cycle, Science, 383(6686), eadf0630, https://doi.org/10.1126/science.adf0630, 2024.

Kunert, N., Aparecido, L. M. T., Wolff, S., Higuchi, N., dos Santos, J., de Araujo, A. C., and Trumbore, S.: A revised hydrological model for the Central Amazon: The importance of emergent canopy trees in the forest water budget, Agric. For. Meteorol., 239, 47-57, https://doi.org/10.1016/j.agrformet.2017.03.002, 2017.

Le Mouël, J. L., Gibert, D., and Poirier, J. P.: On transient electric potential variations in a standing tree and atmospheric electricity, CR Géosci., 342(2), 95-99, https://doi.org/10.1016/j.crte.2009.12.001, 2010.

Le Mouël, J. L., Gibert, D., Boulé, J. B., Zuddas, P., Courtillot, V., Lopes, F., ... and Maineult, A.: On the effect of the luni-solar gravitational attraction on trees, arXiv [preprint], arXiv: 2402.07766, doi:10.48550/arXiv.2402.07766, 12 February 2024.

Leroy, P., Devau, N., Revil, A., and Bizi, M.: Influence of surface conductivity on the apparent zeta potential of amorphous silica nanoparticles, J. Colloid Interf. Sci., 410, 81-93, https://doi.org/10.1016/j.jcis.2013.08.012, 2013.

Linde, N., Revil, A., Boleve, A., Dagès, C., Castermant, J., Suski, B., and Voltz, M.: Estimation of the water table throughout a catchment using self-potential and piezometric data in a Bayesian framework, J. Hydrol., 334(1), 88–98. https://doi.org/10.1016/j.jhydrol.2006.09.027, 2007.

Linde, N., Doetsch, J., Jougnot, D., Genoni, O., Dürst, Y., Minsley, B. J., ... and Luster, J.: Self-potential investigations of a gravel bar in a restored river corridor, Hydrol. Earth Syst. Sci., 15, 729-742, https://doi.org/10.5194/hess-15-729-2011, 2011.

Loiseau, B., Carrière, S. D., Jougnot, D., Singha, K., Mary, B., Delpierre, N., ... and Martin-StPaul, N. K.: The geophysical toolbox applied to forest ecosystems–A review, Sci. Total Environ., 899, 165503, https://doi.org/10.1016/j.scitotenv.2023.165503, 2023.

López-Portillo, J., Ewers, F. W., and Angeles, G.: Sap salinity effects on xylem conductivity in two mangrove species, Plant Cell Environ., 28, 1285–1292, https://doi.org/10.1111/j.1365-3040.2005.01366.x, 2005.

Losso, A., Gauthey, A., Choat, B., and Mayr, S.: Seasonal variation in the xylem sap composition of six Australian trees and shrubs, AoB Plants, 15(5), plad064, https://doi.org/10.1093/aobpla/plad064, 2023.

Love, C. J., Zhang, S., and Mershin, A.: Source of sustained voltage difference between the xylem of a potted Ficus benjamina tree and its soil, PloS one, 3(8), e2963, https://doi.org/10.1371/journal.pone.0002963, 2008.

Luo, Z., Deng, Z., Singha, K., Zhang, X., Liu, N., Zhou, Y., ... and Guan, H.: Temporal and spatial variation in water content within living tree stems determined by electrical resistivity tomography, Agric. For. Meteorol., 291, 108058, https://doi.org/10.1016/j.agrformet.2020.108058, 2020.

McDonald, K. C., Zimmermann, R., and Kimball, J. S.: Diurnal and spatial variation of xylem dielectric constant in Norway spruce (Picea abies [L.] Karst.) as related to microclimate, xylem sap flow, and xylem chemistry, IEEE Trans. Geosci. Remote Sens., 40(9), 2063-2082, https://doi.org/10.1109/TGRS.2002.803737, 2002.

Miller, A. J., and Wells, D. M.: Electrochemical Methods and Measuring Transmembrane Ion Gradients, in: Plant Electrophysiology: Theory and Methods, edited by Volkov, A. G., Springer, Berlin, Heidelberg, Germany, 15-34, https://doi.org/10.1007/978-3-540-37843-3_2, 2006.

Moreno, M., Simioni, G., Cailleret, M., Ruffault, J., Badel, E., Carrière, S., ... and Martin-StPaul, N.: Consistently lower sap velocity and growth over nine years of rainfall exclusion in a Mediterranean mixed pine-oak forest, Agric. For. Meteorol., 308, 108472, https://doi.org/10.1016/j.agrformet.2021.108472, 2021.

Mottl, O., Flantua, S. G., Bhatta, K. P., Felde, V. A., Giesecke, T., Goring, S., ... and Williams, J. W.: Global acceleration in rates of vegetation change over the past 18,000 years, Science, 372(6544), 860-864, https://doi.org/10.1126/science.abg1685, 2021.

Nardini A., Salleo S., and Jansen S.: More than just a vulnerable pipeline: xylem physiology in the light of ion-mediated regulation of plant water transport, J. Exp. Bot., 62, 4701–4718, https://doi.org/10.1093/jxb/err208, 2011.

Nobel, P. S. (Eds): Physicochemical and Environmental Plant Physiology. Academic Press, ISBN 978-0-12-374143-1, 2009.

Nolan, C., Overpeck, J. T., Allen, J. R., Anderson, P. M., Betancourt, J. L., Binney, H. A., ... and Jackson, S. T.: Past and future global transformation of terrestrial ecosystems under climate change, Science, 361(6405), 920-923, https://doi.org/10.1126/science.aan5360, 2018.

Oki, T., and Kanae, S.: Global hydrological cycles and world water resources, Science, 313(5790), 1068-1072, https://doi.org/10.1126/science.1128845, 2006.

Ollivier, C., Olioso, A., Carrière, S. D., Boulet, G., Chalikakis, K., Chanzy, A., ... and Weiss, M.: An evapotranspiration model driven by remote sensing data for assessing groundwater resource in karst watershed, Sci. Total Environ., 781, 146706, https://doi.org/10.1016/j.scitotenv.2021.146706, 2021.

Oliveras, I., and Llorens, P.: Medium-term sap flux monitoring in a Scots pine stand: analysis of the operability of the heat dissipation method for hydrological purposes, Tree Physiol., 21(7), 473-480, https://doi.org/10.1093/treephys/21.7.473, 2001.

Oyarce, P., and Gurovich, L.: Electrical signals in avocado trees: Responses to light and water availability conditions, Plant Signal. Behav., 5(1), 34-41, https://doi.org/10.4161/psb.5.1.10157, 2010.

Perrier, F. E., Petiau, G., Clerc, G., Bogorodsky, V., Erkul, E., Jouniaux, L., ... and Yazici-Cakin, O.: A one-year systematic study of electrodes for long period measurements of the electric field in geophysical environments, Journal of Geomagnetism and Geoelectricity, 49(11-12), 1677-1696, https://doi.org/10.5636/jgg.49.1677, 1997.

Petiau, G.: Second generation of lead-lead chloride electrodes for geophysical applications, Pure Appl. Geophys., 157, 357-382, https://doi.org/10.1007/s000240050004, 2000.

Poyatos, R., Granda, V., Molowny-Horas, R., Mencuccini, M., Steppe, K., and Martínez-Vilalta, J.: SAPFLUXNET: towards a global database of sap flow measurements, Tree Physiol., 36(12), 1449-1455, https://doi.org/10.1093/treephys/tpw110, 2016.

Poyatos, R., Granda, V., Flo, V., Adams, M. A., Adorján, B., Aguadé, D., ... and Van Der Tol, C.: Global transpiration data from sap flow measurements: the SAPFLUXNET database, Earth Syst. Sci. Data Discuss., 13, 2607–2649, https://doi.org/10.5194/essd-13-2607-2021, 2021.

Pozdnyakov, A. I.: Bioelectric potentials in the soil-plant system, Eurasian Soil Sci., 46, 742-750, https://doi.org/10.1134/S1064229313070089, 2013.

Revil, A., Pezard, P.A., and Glover, P.W.J.: Streaming potential in porous media: 1. Theory of the zeta potential, J. Geophys. Res. Solid Earth, 104(B9), 20021-20031, https://doi.org/10.1029/1999JB900089, 1999.

Revil, A., and Jardani, A. (Eds): The Self-potential Method: Theory and Applications in Environmental Geosciences. Cambridge University Press, ISBN 978-1-107-01927-0, 2013.

Schill, V., Hartung, W., Orthen, B., and Weisenseel, M. H.: The xylem sap of maple (*Acer platanoides*) trees—sap obtained by a novel method shows changes with season and height, J. Exp. Bot., 47(294), 123-133, https://doi.org/10.1093/jxb/47.1.123, 1996.

Schlesinger, W. H., and Jasechko, S.: Transpiration in the global water cycle, Agric. For. Meteorol., 189, 115-117, https://doi.org/10.1016/j.agrformet.2014.01.011, 2014.

Smith, D. M., and Allen, S. J.: Measurement of sap flow in plant stems, J. Exp. Bot., 47(12), 1833-1844, 1996.

Simioni, G., Marie, G., Davi, H., Martin-St Paul, N., and Huc, R.: Natural forest dynamics have more influence than climate change on the net ecosystem production of a mixed Mediterranean forest, Ecol. Modell., 416, 108921, https://doi.org/10.1016/j.ecolmodel.2019.108921, 2020.

Spanswick, R. M.: Electrogenic pumps. in: Plant Electrophysiology: Theory and Methods, edited by Volkov, A. G., Springer, Berlin, Heidelberg, Germany, 221-246, https://doi.org/10.1007/978-3-540-37843-3_10, 2006.

Sperry, J. S.: Evolution of water transport and xylem structure, Int. J. Plant Sci., 164(S3), S115-S127, https://doi.org/10.1086/368398, 2003.

Steinberg, S. L., McFarland, M. J., and Worthington, J. W.: Comparison of trunk and branch sap flow with canopy transpiration in pecan, J. Exp. Bot, 41(6), 653-659, https://doi.org/10.1093/jxb/41.6.653, 1990.

Steppe, K., and Lemeur, R.: Effects of ring-porous and diffuse-porous stem wood anatomy on the hydraulic parameters used in a water flow and storage model, Tree Physiol., 27(1), 43-52, https://doi.org/10.1093/treephys/27.1.43, 2007.

Tattar, T. A., and Blanchard, R. O.: Electrophysiological research in plant pathology, Annu. Rev. Phytopathol., 14(1), 309-325, https://doi.org/10.1146/annurev.py.14.090176.001521, 1976.

Torrence, C., and Compo, G. P.: A practical guide to wavelet analysis, Bull. Am. Meteorol. Soc., 79(1), 61-78, https://doi.org/10.1175/1520-0477(1998)079%3C0061:APGTWA%3E2.0.CO;2, 1998.

Valois, R., Galibert, P. Y., Guerin, R., and Plagnes, V.: Application of combined time-lapse seismic refraction and electrical resistivity tomography to the analysis of infiltration and dissolution processes in the epikarst of the Causse du Larzac (France), Near Surf. Geophys., 14(1), 13-22, https://doi.org/10.3997/1873-0604.2015052, 2016.

Volkov, A. G., and Markin, V. S.: Phytosensors and Phytoactuators, in: Plant Electrophysiology: Signaling and Responses, edited by: Volkov, A. G., Springer, Berlin, Heidelberg, Germany, 173-206, https://doi.org/10.1007/978-3-642-29110-4_7, 2012.

Voytek, E. B., Barnard, H. R., Jougnot, D., and Singha, K.: Transpiration-and precipitation-induced subsurface water flow observed using the self-potential method, Hydrol. Process., 33(13), 1784-1801, https://doi.org/10.1002/hyp.13453, 2019.

Wang, J., Turner, N. C., Feng, H., Dyck, M., and He, H.: Heat tracer-based sap flow methods for tree transpiration measurements: a mini review and bibliometric analysis, J. Exp. Bot., 74(3), 723-742, https://doi.org/10.1093/jxb/erac424, 2023.

Wei, Z., Yoshimura, K., Wang, L., Miralles, D. G., Jasechko, S., and Lee, X.: Revisiting the contribution of transpiration to global terrestrial evapotranspiration, Geophys. Res. Lett., 44(6), 2792-2801, https://doi.org/10.1002/2016GL072235, 2017.

https://doi.org/10.5194/hess-2024-240
Preprint. Discussion started: 23 September 2024

Zapata, R., Oliver-Villanueva, J. V., Lemus-Zúñiga, L. G., Luzuriaga, J. E., Mateo Pla, M. A., and Urchueguía, J. F.: Evaluation of electrical signals in pine trees in a mediterranean forest ecosystem, Plant Signal. Behav., 15(10), 1795580, https://doi.org/10.1080/15592324.2020.1795580, 2020.

Zapata, R., Oliver-Villanueva, J. V., Lemus-Zúñiga, L. G., Fuente, D., Mateo Pla, M. A., Luzuriaga, J. E., and Moreno Esteve, J. C.: Seasonal variations of electrical signals of Pinus halepensis Mill. in Mediterranean forests in dependence on climatic conditions, Plant Signal. Behav., 16(10), 1948744, https://doi.org/10.1080/15592324.2021.1948744, 2021.